Structure, Deprotonation Energy, and Cation Affinity of an Ethynyl-Expanded Cubane

Steven M. Bachrach*

Department of Chemistry, Trinity University, 715 Stadium Drive, San Antonio, Texas 78212

Received: February 17, 2003; In Final Form: March 20, 2003

Ⓦ **This paper contains enhanced objects available on the Internet at http://pubs.acs.org/jpcafh.**

The ethynyl-expanded cubane **2** is examined at the B3LYP/6-31G* level for its structure, ring-strain energy, deprotonation energy, and affinity toward lithium and sodium cation. The estimate of the ring-strain energy of **2** is 48.3 kcal mol^{-1}. Its free energy of deprotonation is 325 kcal mol^{-1}. Lithium cation coordinates to the face of **2**, while sodium coordinates to the cage center. These properties are compared with those of simple acyclic alkynes and cyclododeca-1,4,7,10-tetrayne, the analogue of the face of **2**.

Diederich and co-workers have been pursuing the synthesis and properties of buta-1,3-diynediyl-expanded molecules.[1] These compounds may possess novel opticoelectronic properties. They recently reported the preparation of the expanded cubane **1**.[2]

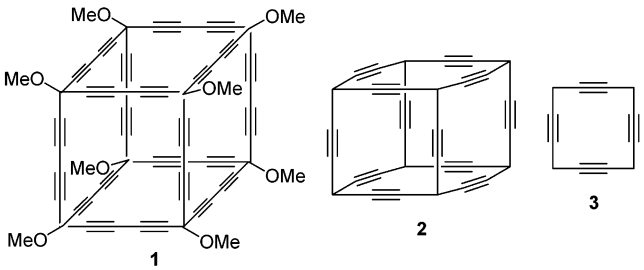

This molecule combines the notion of a conjugated π-system and the Platonic solids. In this paper, we discuss ab initio and density function theory (DFT) computations of the ethynyl-expanded cubane **2**, a simpler analogue of **1**. In particular, we address its structure, ring-strain energy (RSE), deprotonation energy (DPE), and cation affinity.

Computational Methods

All structures were completely optimized within given point groups. All neutral species were optimized at B3LYP/6-31G*. To determine DPE, it is necessary to include diffuse functions,[3−5] so all species were reoptimized at B3LYP/6-31+G*.[6] There have been problems reported with using B3LYP/6-31+G* for computing deprotonation energies.[5] MP2/6-31+G* computations can provide excellent DPEs for hydrocarbons, because of fortuitous cancellation of errors, and some are reported here. The relatively good agreement between the B3LYP and MP2 results reported here are also likely due to fortuitous cancellation of errors at the B3LYP level. Unfortunately, we do not have the computing resources necessary to handle MP2/6-31+G* calculations of **2** and its conjugate base.

The nature of all structures was ascertained with analytical frequencies, which were used without scaling to compute 298 K thermal contributions to free energies using standard partition-function approximations.[7] Because of the size of the computation, it was unfeasible to compute analytical frequencies of **2** and its conjugate base at B3LYP/6-31+G*, though we were able to optimize both structures at this level. We have used the B3LYP/6-31G* frequencies to correct the B3LYP/6-31+G* results for **2** and its conjugate base. This approximation is likely to be quite adequate; for the other alkynes and their conjugates bases studied here, the differences in the free energies calculated with the B3LYP/6-31G* and the B3LYP/6-31+G* frequencies are less than 0.4 kcal mol^{-1}. All computations were performed using Gaussian 98.[8]

Results and Discussion

Structure and Ring-Strain Energy. The optimized structure of **2** possesses O_h symmetry and is shown in Figure 1. The geometry is essentially identical when optimized at B3LYP/6-31G* and B3LYP/6-31+G*.

To evaluate this geometry, a number of reference compounds were examined and their structures, along with important geometric parameters, are drawn in Figure 1. We note in passing that the computed geometry of propyne is in excellent agreement with the structure obtained via microwave spectroscopy.[9] On the basis of the structures of the acyclic, unstrained alkynes, one can ascertain that the normal C≡C distance is about 1.21 Å and the normal C−C$_{sp}$ distance is 1.46 Å (lengthening slightly with substitution about the saturated carbon) with a linear arrangement about the sp carbon atom. Cyclododeca-1,4,7,10-tetrayne (**3**) is an analogue of a face of **2**. Its C≡C distance is quite normal, and its C−C distance compares favorably with that in pent-1,4-diyne, which is also disubstituted at the saturated carbon. However, the angle about the sp carbon is decidedly bent, being an angle of 170.8°.

The triple bond distance in **2** is essentially identical to the lengths in the reference compounds. The C−C bond is slightly longer than any of the reference compounds, including that of 3-ethynylpenta-1,4-diyne, which also has a tertiary saturated carbon. However, its angle about the sp carbon differs quite obviously from the others—it is 166.4°. This distortion from linearity is clearly a manifestation of the strain in this cube.

We employ the group equivalent schema[10] to evaluate the ring-strain energy. To place the RSE of **2** in perspective, we also evaluate the RSE of cubane and **3**. The group equivalent reactions used are shown in Scheme 1, and the RSE is the

* To whom correspondence should be addressed. E-mail: sbachrach@trinity.edu.

10.1021/jp034406k CCC: $25.00
Published on Web 05/22/2003

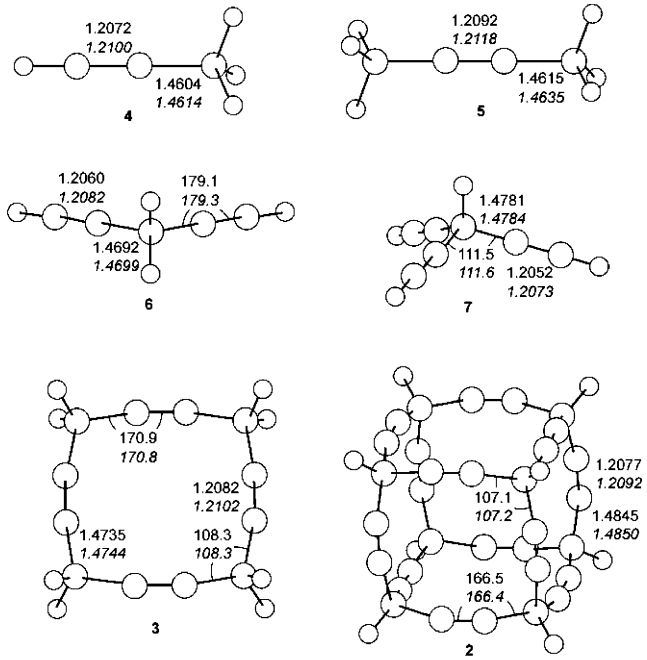

Figure 1. Geometries of **2**−**7**. All distances are in Å, and all angles are in deg. B3LYP/6-31G* results are on top, and B3LYP/6-31+G* results are on bottom and in italics. Carbon atoms are indicated as large circles and hydrogen atoms as small circles.

Ⓦ A rotatable image of **2** in MOL format viewable in RasMol is available.

SCHEME 1

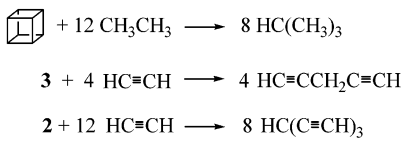

TABLE 1: RSE (kcal mol^{-1}) Evaluated Using Scheme 1

compound	B3LYP/6-31G*	B3LYP/6-31+G*
cubane	140.3	138.4
3	9.5	9.3
2	51.0	48.3

negative of the energy of these reactions. The values of the RSE (computed using the electronic energies corrected for zero-point energy (ZPE)) are listed in Table 1.

Cubane **8** is quite strained, its RSE being estimated here as about 140 kcal mol^{-1}, somewhat less than previous estimates.[11] The analogue of a face of the expanded cube **2** is **3**, and this ring is relatively unstrained; its RSE is about 9 kcal mol^{-1}. Because this is much less than the strain of cyclobutane (the analogue of a face of cubane), the strain of **2** should be much less than the strain of cubane. This is in fact true; the RSE of **2** is about 50 kcal mol^{-1}. The large strain in cubane is due principally to angle strain because its angles about carbon are 90°. Insertion of the ethynyl group into the C−C bonds giving **2** allows the angles to expand to 107.1°, quite near a normal tetrahedral angle. This expansion comes about with a penalty—contraction of the angles about the alkynyl carbons from 180° to 166.4°. We estimate this penalty by optimizing 2-butyne with both C−C−C angles restricted to that in **2**, that is, 166.4°, and comparing it to the energy of linear 2-butyne. At B3LYP/6-31+G* this difference is 1.76 kcal mol^{-1}. Therefore, because there are 12 such bent triple bonds in **2**, about 20 kcal mol^{-1} of the RSE of **2** can be attributed to the strain about its triple bonds.

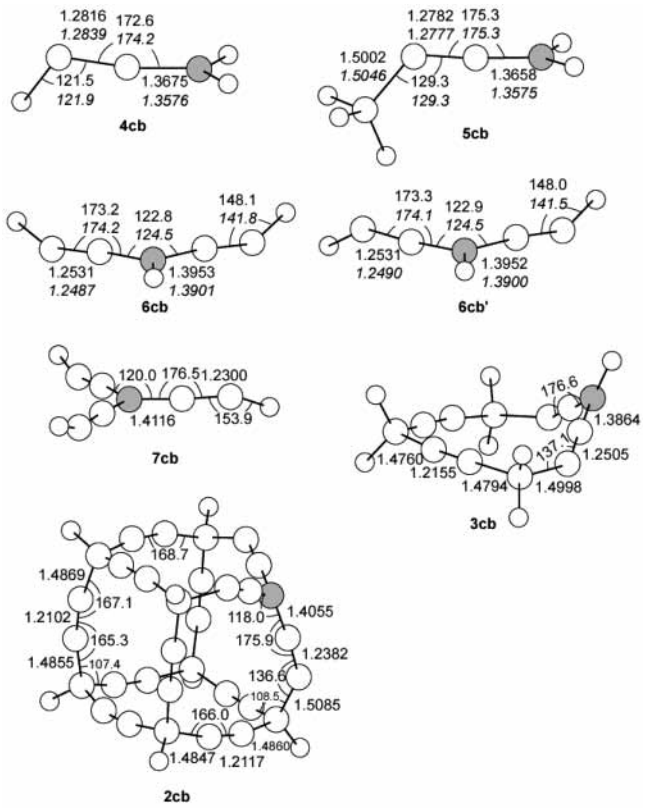

Figure 2. Geometries of **2cb**−**7cb**. All distances are in Å, and all angles are in deg. MP2/6-31+G* results are on top, and B3LYP/6-31+G* results are on bottom and in italics. Carbon atoms are indicated as large circles and hydrogen atoms as small circles. The deprotonated carbon is indicated as the shaded circle.

Ⓦ A rotatable image of **2cb** in MOL format viewable in RasMol is available.

Deprotonation Energy. An interesting consequence of strained species is their enhanced acidity. For example, the free energies for deprotonation of propane, cyclobutane, cyclopropane, and cubane are 419.4, 408.4, 401, and 396.5 kcal mol^{-1}, respectively.[12−14] This suggests that **2** should be relatively acidic. Additionally, protons adjacent to triple bonds express enhanced acidity; for example, $\Delta G°$ for the deprotonation of 2-butyne is 381.5 kcal mol^{-1}.[15] We anticipate that **2** should be quite acidic.

To place the acidity of **2** in proper context, we examine the deprotonation energies of some model compounds: the acyclic alkynes propyne **4**, 2-butyne **5**, pent-1,4-diyne **6**, 3-ethynylpenta-1,4-diyne **7**, cyclododeca-1,4,7,10-tetrayne **3**, and cubane **8**. For the acyclic alkynes, we deprotonate the saturated carbon (the propargylic proton), which is analogous to the saturated center of **2**.[16] Deprotonation leads to the corresponding conjugate bases, labeled as **2cb**−**7cb**, and their structures, along with important geometric parameters, are drawn in Figure 2. The DPEs are listed in Table 2.

We first examine the structure of the conjugate bases. Deprotonation of the propargylic position results in an anion having two resonance structures, shown in Scheme 2. Structure **9A** has anion formally on what was the sp^3 carbon, while structure **9B** is an allenic system with the anion on what was a carbon of the triple bond but is now rehybridized to sp^2. This latter resonance structure is likely to predominate because of the lone pair electrons occupying an orbital with greater s-character. Thus, we anticipate the bent geometry of **9B** for the conjugate bases. Examination of Figure 2 confirms the dominance of the **9B** resonance structure. Using the label C_t

TABLE 2: Free Energy (kcal mol^{-1}) for Deprotonation

	ΔG		
compound	B3LYP/6-31+G*	MP2/6-31+G*	expt
cubane **8**	399.8	397.6	396.5[a]
propyne **4**	371.6	377.1	
2-butyne **5**	377.8	382.5	381.5[b]
pent-1,4-diyne **6**	347.2, 346.8	354.1, 353.7	
3-ethynylpenta-1,4-diyne **7**	325.9	334.1	
cyclododeca-1,4,7,10-tetrayne **3**	346.2		
2	316.1		

[a] Reference 14. [b] Reference 15.

SCHEME 2

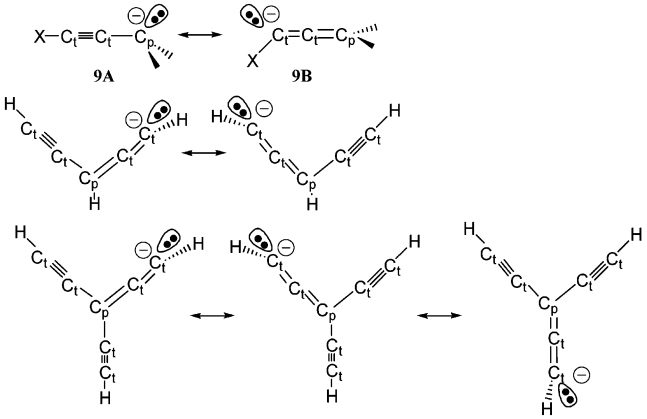

SCHEME 3

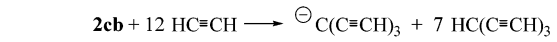

and C_p to indicate the former alkynyl and propargyl carbons, respectively, we note the near perfect sp^2 angle H−C_t−C_t in **4cb**. This angle opens up slightly to 129.3° in **5cb**. Addition of more alkynyl groups to the saturated carbon results in further widening of this angle: 148° in **6cb** and 159.5° in **7cb**. (We note in passing that there are two conformational isomers of **6cb**, having C_s and C_2 symmetry, which are of nearly identical energy.) This suggests that increasing alkynyl substitution leads to delocalization of the anion into each of the alkynyl groups, resulting in less negative charge on each terminal carbon and thereby lessening its sp^2 character and increasing its sp character (see the resonance structures for **6cb** and **7cb** in Scheme 2). The decreasing C_t−C_t bond length (1.284 Å in **4cb**, 1.249 Å in **6cb**, and 1.230 Å in **7cb**) and increasing C_p−C_t bond length (1.358 Å in **4cb**, 1.390 Å in **6cb**, and 1.412 Å in **7cb**) with increasing alkynyl substitution corroborates this resonance picture.

The conjugate bases of the alkynyl-expanded rings follow this same behavior. Deprotonation of **3** results in a structure (**3cb**) with only C_s symmetry. The deprotonated carbon is nearly planar (the sum of the angles at this atom is 358.5°), and the C_p−C_t and C_t−C_t bond distances are very similar to those in **6cb**. The C−C_t−C_t angle is 137.1°, expressing significant sp^2 character. Deprotonation of the expanded cubane results in **2cb**, which has C_{3v} symmetry. Again, the deprotonated carbon is nearly planar (the angle sum about the atom is 354.1°), which requires significant distortion from its former cubic shape—the anionic corner is squashed inward. The C_p−C_t and C_t−C_t bond distances of **2cb** are 1.406 and 1.238 Å, respectively, very similar to the corresponding distances in the acyclic model compound **7cb**. The odd shape of **2cb** might imply some serious strain, perhaps suppressing the acidity of **2**. The RSE of **2cb**, estimated using the reaction shown in Scheme 3, is 39.2 kcal mol^{-1}. This conjugate base is therefore *less* strained than its neutral acid. The substantial geometric changes that accompany deprotonation, especially the rehybridization of the alkynyl centers, result in the lower strain energy of the conjugate base. Strain relief will accompany the loss of a proton from **2**, enhancing its acidity.

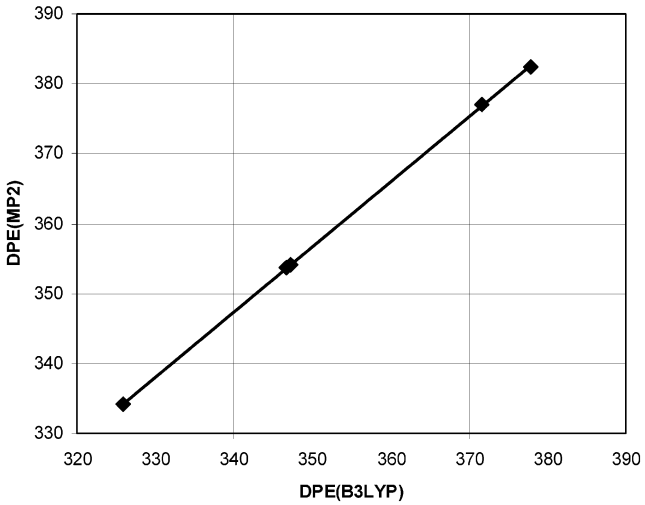

Figure 3. Correlation of DPEs (kcal mol^{-1}) computed at B3LYP/6-31+G* and MP2/6-31+G*.

We now turn to the energetics of deprotonation. Merrill and Kass[5] have noted that MP2/6-31+G* DPEs are in excellent agreement with experiment for a series of hydrocarbons, thanks to fortuitous cancellation of errors due to a small basis set and limited accounting of electron correlation. We find the MP2/6-31+G* free energy of deprotonation for cubane and 2-butyne to again be in fine agreement with experiment; the error is about 1 kcal mol^{-1}. Merrill and Kass[5] also point out that B3LYP DPEs have large errors (5−7 kcal mol^{-1}) when small basis sets are employed, and because of the size of the systems under study here, especially **2** and **3**, we are limited to using the 6-31+G* basis. The B3LYP/6-31+G* estimate for the DPE of cubane is 2 kcal mol^{-1} above the MP2 value and that of 2-butyne is 4.7 kcal mol^{-1} below the MP2 value. Therefore, we expect that the B3LYP values will have an error of about 5 kcal mol^{-1}, so we must focus on trends rather than absolute values.

Examination of the MP2 DPEs for the series propyne, pent-1,4-diyne, and 3-ethynylpenta-1,4-diyne probes the effect of alkynyl substitution. Addition of an ethynyl group to propyne reduces its DPE by 23.4 kcal mol^{-1}, and the second additional ethynyl group further reduces the DPE by 19.6 kcal mol^{-1}. While the DPE values at B3LYP are all less than those determined at MP2, the differences in DPEs due to ethynyl substitution are of almost identical size as those computed at MP2. In fact, as shown in Figure 3, the MP2 and B3LYP estimates of the DPE of **4**−**7** are well-correlated by the relationship

$$\Delta G(\mathrm{MP2}) = 0.936\Delta G(\mathrm{B3LYP}) + 29.3 \qquad (1)$$

having $r^2 = 0.999$. Each ethynyl group allows for delocalization of the anion as shown in Scheme 2. This delocalization stabilizes the anion and therefore leads to a reduced DPE.

The DPE of **3** is estimated to be 346.2 kcal mol^{-1} at B3LYP/6-31+G*. Correcting for the systematic underestimation at B3LYP using eq 1 gives a DPE of 353 kcal mol^{-1}. This is about the same value as that for **6**, the acyclic analogue of **3**. Because the RSE of **3** is small, the similar DPEs of **3** and **6** are expected

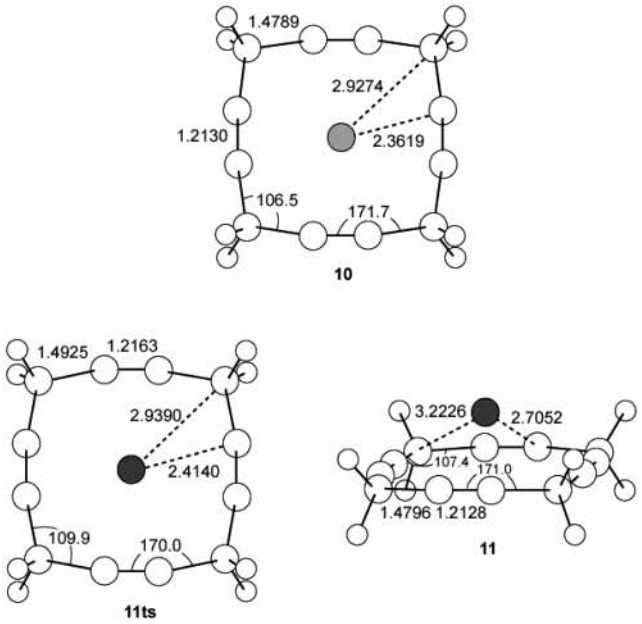

Figure 4. B3LYP/6-31G* geometries of the Li^+ and Na^+ complexes with **3**. All distances are in Å, and all angles are in deg. Carbon atoms are indicated as large circles and hydrogen atoms as small circles. Li and Na are denoted by a light and dark shaded circles, respectively.

TABLE 3: Free Energy (kcal mol^{-1}) of Cation Complexation at B3LYP/6-31G*

complex	ΔG
10	−60.0
11	−38.7
11ts	−26.1
12	−60.3
12ts	−55.1
13i	−52.5
13o	−39.8
13ts	−27.1

because the dominant factor determining their acidities is the same—the delocalization of the anion into two ethynyl groups.

The B3LYP estimate for the DPE of **2** is 316.1 kcal mol^{-1}. Correcting again, using eq 1, for the error in this method gives a value of about 325 kcal mol^{-1}. This value is decidedly smaller (about 10 kcal mol^{-1}) than the DPE of its acyclic analogue 3-ethynylpenta-1,4-diyne **7**. Delocalization into the three ethynyl groups is not the only factor at play here. **2** is fairly strained, and strained ring systems have enhanced acidity due to the increased s-character in their C−H bonds. Just as the acidity of cubane is enhanced relative to acyclic hydrocarbons, the strain in **2** increases the s-character in its C−H bonds. The DPE of **2** is about 70 kcal mol^{-1} less than that of cubane and about 80 kcal mol^{-1} less than that of isobutane (DPE[13] of 405.7 kcal mol^{-1}). The delocalization of charge into the three alkynyl groups clearly is the more dominant of the these two effects. Compounds with similar DPEs include methyl-, fluoro-, and amino-substituted benzoic acids and lysine.[12] The ethynyl-expanded cubane **2** is therefore quite acidic.

Cation Affinity. The host species in complexes with cations typically possess a cavity to hold the guest and available electron pairs to interact with the positive charge. The ethynyl-expanded cubanes appear to meet these qualifications, and therefore, we examined the ability of **2** and its face-analogue **3** to serve as hosts toward small cations, particularly Li^+ and Na^+.

In Figure 4, we draw the structures of the complexes of **3** with Li^+ (**10**) and Na^+ (**11**). Complexation energies are listed in Table 3. The closest distance between carbon atoms across the ring is 4.592 Å. Subtracting off twice the van der Waals radius of carbon gives a hole of diameter 1.3 Å. The small lithium cation can fit within this hole, and thus, the most stable structure has the lithium cation lying in the center of the ring. The complex **10** has D_{4h} symmetry. The triple-bonded carbons actually move inward in the complex relative to the free ring, as seen in a smaller angle about the saturated carbon and a larger angle about the sp carbons. The free energy of complexation to form **10** is −60.0 kcal mol^{-1}.

The center of the ring of **3** is not large enough to hold the sodium cation. The triple bonds have to bow out to accommodate the sodium cation in the D_{4h} complex of **3** with Na^+ (**11ts**). The angle about the saturated carbon is 3.4° wider in **11ts** than in **10**, and the distance between the cation and the triple-bonded carbons is 0.05 Å shorter in **10** than in **11ts**. **11ts** has one imaginary frequency, corresponding to motion of Na^+ out of the ring plane. The local energy minimum for the complex is **11**, in which sodium lies above the ring. The carbon atoms of the ring are nearly coplanar, and sodium lies 1.318 Å above the ring midpoint. The transition state for sodium passing through the ring (**11ts**) is 12.6 kcal mol^{-1} above **11**. The free energy for complexation to form **11** is −38.7 kcal mol^{-1}. This is some 20 kcal mol^{-1} less than that for complexation of Li^+, which reflects the smaller atom's better fit inside the ring. Further, because the charge density is greater on the smaller (Li) cation, the larger cation (Na) will have the lower affinity given the same number of coordination sites with the host.

Because the lithium cation can fit inside **3**, it can surely fit inside **2**. Optimization of the complex of **2** and Li^+ within O_h symmetry leads to the structure **12ts**, which has three imaginary frequencies, corresponding to motion of lithium toward any of the faces of the cube. Reducing the symmetry to C_{4v} and reoptimizing produces **12**, in which the cation lies just outside one of the faces. This face is only slightly enlarged relative to the other five faces. The distances from Li to the carbon atoms of this face are comparable to those in **10**, even though the ring is strictly planar in **10** and slightly puckered in **12**. These structures are drawn in Figure 5.

The complexation free energy (Table 3) to produce **12** is −60.3 kcal mol^{-1}. This is essentially identical to the complex energy for **10**, which is logical because in both structures the lithium cation is associated with one 12-membered ring. **12ts**, having the cation in the center of the cage, is 5.2 kcal mol^{-1} less stable than **12**, reflecting the favorable interactions present when the small lithium cation sits directly in a face.

Sodium cation is too large to sit within **3**, but it is small enough to fit within the cavity of the expanded cubane **2**. The O_h structure **13i** (see Figure 5 and Table 3) with the sodium cation at the center of the cage is a local energy minimum. The geometry of the cage is little changed by the addition of the sodium cation to its center. The free energy of formation of this complex is −52.5 kcal mol^{-1}, very nearly the same as that for forming the Li^+ analogue **12ts**.

Because the complex of Na^+ with **3** has the cation above the ring, another structure for the complex of Na^+ with **2** is possible, this one of C_{4v} symmetry with the cation sitting outside the cage positioned above the middle of a face. This structure **13o**, drawn in Figure 5, is a local energy minimum. The cation lies 1.424 Å above the middle of one of the faces. This is slightly farther out than that in **11**, but the face of the expanded cubane is more puckered than that in **11**, so direct comparison is somewhat vague. The complexation energy of **13o** is −39.8 kcal mol^{-1}, which is within 1 kcal mol^{-1} of the complexation

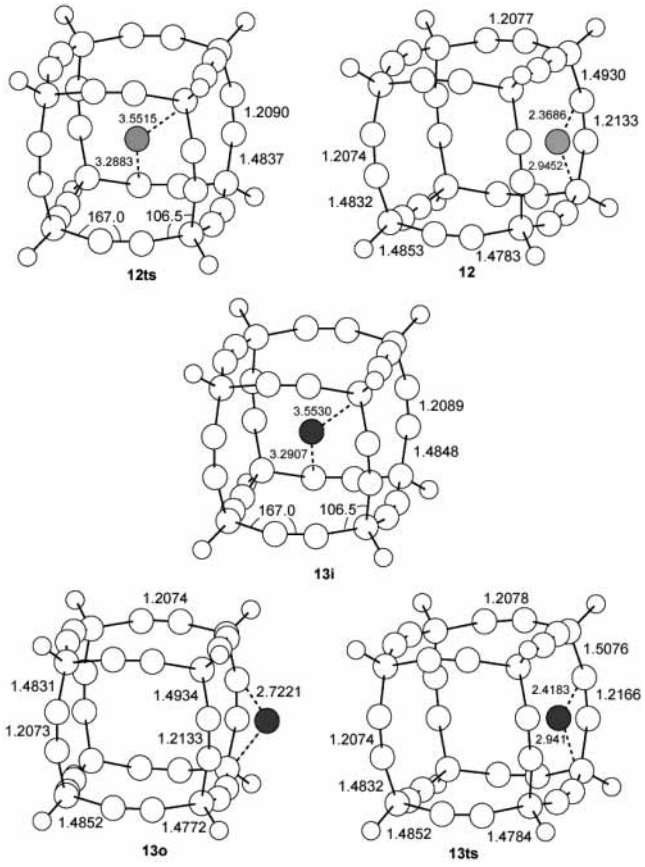

Figure 5. B3LYP/6-31G* geometries of the Li^+ and Na^+ complexes with **2**. All distances are in Å, and all angles are in deg. Carbon atoms are indicated as large circles and hydrogen atoms as small circles. Li and Na are denoted by a light and dark shaded circles, respectively.

of **11**. The interactions between the hydrocarbon and the cation are identical in both complexes.

A transition state separates the two sodium complexes with **2**. This transition state has C_{4v} symmetry with the cation positioned for passage through the center of a face. **13ts** is structurally similar to **11ts**, which is the transition state for passage of the cation through the center of **3**. This transition state is 25.4 kcal mol^{-1} above **13i**. It is 12.7 kcal mol^{-1} above **13o**, which is nearly identical to the energy difference between **11** and **11ts**, the analogue of its face.

The ethynyl-expanded cubane **2** can therefore act as a host toward both lithium and sodium cations. The mode of complexation is different for the two cations: face-centered for the smaller lithium cation and inside the cage for the larger sodium cation.

Conclusion

The ethynyl-expanded cubane **2** has a relatively small ring-strain energy of 48.3 kcal mol^{-1}. This ring strain and the ability of the anion of the resulting conjugate base to delocalize into three adjacent alkylyl groups lead to the extraordinary acidity of **2**; $\Delta G°$ of deprotonation of **2** is estimated to be 325 kcal mol^{-1}, some 70 kcal mol^{-1} less than the DPE of cubane. Last, **2** is predicted to act as a host toward lithium and sodium cations. Lithium cation will coordinate to a face of **2**, while sodium cation prefers the center of the cage. We hope that these predictions will encourage experimental exploration of the properties of this novel hydrocarbon.

Supporting Information Available: Coordinates of all optimized B3LYP/6-31+G* or B3LYP/6-31G* structures, their absolute energies, and number of imaginary frequencies. This material is available free of charge via the Internet at http://pubs.acs.org.

References and Notes

(1) (a) Boldi, A. M.; Diederich, F. *Angew. Chem., Int. Ed. Engl.* **1994**, *33*, 468−471. (b) Nielsen, M. B.; Schreiber, M.; Baek, Y. G.; Seiler, P.; Lecomte, S.; Boudon, C.; Tykwinski, R. R.; Gisselbrecht, J. P.; Gramlich, V.; Skinner, P. J.; Bosshard, C.; Gunter, P.; Gross, M.; Diederich, F. *Chem.—Eur. J.* **2001**, *7*, 3263−3280. (c) Diederich, F. *Chem. Commun.* **2001**, 219−227.

(2) Manini, P.; Amrein, W.; Gramlich, V.; Diederich, F. *Angew. Chem., Int. Ed.* **2002**, *41*, 4339−4343.

(3) Chandrasekhar, J.; Andrade, J. G.; Schleyer, P. v. R. *J. Am. Chem. Soc.* **1981**, *103*, 5609−5612.

(4) Saunders, W. H., Jr. *J. Phys. Org. Chem.* **1994**, *7*, 268−271.

(5) Merrill, G. N.; Kass, S. R. *J. Phys. Chem.* **1996**, *100*, 17465−17471.

(6) (a) Becke, A. D. *J. Chem. Phys.* **1993**, *98*, 5648−5650. (b) Lee, C.; Yang, W.; Parr, R. G. *Phys. Rev. B* **1988**, *37*, 785−789. (c) Vosko, S. H.; Wilk, L.; Nusair, M. *Can. J. Phys.* **1980**, *58*, 1200−1211. (d) Stephens, P. J.; Devlin, F. J.; Chabalowski, C. F.; Frisch, M. J. *J. Phys. Chem.* **1994**, *98*, 11623−11627.

(7) Cramer, C. J. *Essentials of Computational Chemistry. Theories and Models*; John Wiley: Chichester, U.K., 2002.

(8) Frisch, M. J.; Trucks, G. W.; Schlegel, H. B.; Scuseria, G. E.; Robb, M. A.; Cheeseman, J. R.; Zakrzewski, V. G.; Montgomery, J. A., Jr.; Stratmann, R. E.; Burant, J. C.; Dapprich, S.; Millam, J. M.; Daniels, A. D.; Kudin, K. N.; Strain, M. C.; Farkas, O.; Tomasi, J.; Barone, V.; Cossi, M.; Cammi, R.; Mennucci, B.; Pomelli, C.; Adamo, C.; Clifford, S.; Ochterski, J.; Petersson, G. A.; Ayala, P. Y.; Cui, Q.; Morokuma, K.; Malick, D. K.; Rabuck, A. D.; Raghavachari, K.; Foresman, J. B.; Cioslowski, J.; Ortiz, J. V.; Stefanov, B. B.; Liu, G.; Liashenko, A.; Piskorz, P.; Komaromi, I.; Gomperts, R.; Martin, R. L.; Fox, D. J.; Keith, T.; Al-Laham, M. A.; Peng, C. Y.; Nanayakkara, A.; Gonzalez, C.; Challacombe, M.; Gill, P. M. W.; Johnson, B. G.; Chen, W.; Wong, M. W.; Andres, J. L.; Head-Gordon, M.; Replogle, E. S.; Pople, J. A. *Gaussian 98*, revision A.7; Gaussian, Inc.: Pittsburgh, PA, 1998.

(9) Debrulle, A.; Boucher, D.; Burie, J.; Demaison, J. *J. Mol. Spectrosc.* **1978**, *72*, 158−164.

(10) Bachrach, S. M. *J. Chem. Educ.* **1990**, *67*, 907−908.

(11) Eaton, P. E. *Angew. Chem., Int. Ed. Engl.* **1992**, *31*, 1421−1436.

(12) Mallard, W. G.; Linstrom, P. J. *NIST Chemistry Webbook*, July 2001 release; National Institute of Standards and Technology: Gaithersburg, MD, 2001.

(13) DePuy, C. D.; Gronert, S.; Barlow, S. E.; Bierbaum, V. M.; Damrauer, R. *J. Am. Chem. Soc.* **1989**, *111*, 1968−1973.

(14) Hare, M.; Emrick, T.; Eaton, P. E.; Kass, S. R. *J. Am. Chem. Soc.* **1997**, *119*, 237−238.

(15) de Visser, S. P.; van der Horst, E.; de Konig, L. J.; van der Hart, W. J.; Nibbering, N. M. M. *J. Mass Spectrom.* **1999**, *34*, 303−310.

(16) (a) For propyne, loss of the acetylenic proton ($\Delta G°$(DPE) = 372.8 kcal mol^{-1} at MP2/6-31+G* and 373.4 kcal mol^{-1} experimentally[16b]) is more favorable than loss of the propargylic proton. However, removal of the propargylic proton is favored over the acetylenic proton in **6** ($\Delta G°$(DPE) = 365.2 kcal mol^{-1} at MP2/6-31+G*) and **7** ($\Delta G°$(DPE) = 360.4 kcal mol^{-1} at MP2/6-31+G*). (b) Robinson, M. S.; Polak, M. L.; Bierbaum, V. M.; DePuy, C. H.; Lineberger, W. C. *J. Am. Chem. Soc.* **1995**, *117*, 6766−6778.